ACI STRUCTURAL JOURNAL TECHNICAL PAPER

Title no. 86-S4

Nonlinear Finite Element Analysis of Reinforced Concrete Membranes

by Frank J. Vecchio

A procedure is described whereby linear elastic finite element routines can be modified to enable nonlinear analysis of reinforced concrete membrane structures. The proposed procedure is based on an iterative, secant stiffness formulation and employs constitutive relations for concrete and reinforcement based on the modified compression field theory. Predictions from the proposed procedure are compared against experimental results, as well as against more complex formulations, and excellent accuracy is found. Example analyses and potential applications of the nonlinear procedure are also described.

Keywords: finite element method; reinforced concrete; secant modulus; stiffness; strains; stresses; **structural analysis;** walls.

In 1981, an international competition was organized to compare analytical methods for predicting the response of reinforced concrete elements subjected to general two-dimensional stress states.[1] Four panels tested in a University of Toronto research program were presented, with the panels' construction, material properties, and loading conditions being simple and well defined. Entrants were asked to predict the panels' ultimate strength and load-deformation response and to describe briefly the basis for their analysis. A total of 27 entries from 13 countries were received, with a strong representation from the leading researchers in the field. Many of the predictions offered were based on analyses conducted using complex nonlinear finite element procedures. Fig. 1 gives an indication of the wide scatter in predictions received. Clearly, the ability to predict response, using finite element procedures or otherwise, was not very good. This collective deficiency was due primarily to a generally poor state of the art in constitutive modeling of cracked reinforced concrete.

The 4 competition panels were part of a series of 30 tested in an extensive research program, from which an analytical model was developed for predicting the response of reinforced concrete membrane elements. The model, known as the modified compression field theory, has been shown to reflect accurately the nonlinear behavior of reinforced concrete[2,3] and now forms the basis for Canadian code[4] procedures for design of reinforced concrete in shear.

Recent efforts at the University of Toronto and elsewhere have been made towards formulating improved finite element procedures for the analysis of more complex structures. Several[5-7] finite element codes have been developed that incorporate the formulations of the modified compression field theory (MCFT), the most comprehensive of which is program FIERCM developed by Stevens et al.[6] Of course, other nonlinear finite element procedures have been developed that are not based on MCFT formulations (e.g., Reference 8 through 10) and these too have met with various degrees of success. With respect to all ongoing developmental work, however, two general observations can be made. First, there is a tendency to favor tangent stiffness formulations as opposed to secant stiffness formulations; discussions of their relative merits can be found in the literature, e.g., Reference 11. Secondly, it is generally perceived that formulations using higher power elements (i.e., multinoded elements with higher order displacement expansions) are preferable to those using simple elements in greater numbers.

In this paper, an alternative nonlinear finite element procedure is presented that incorporates the constitutive relations of the MCFT. Contrary to current preferences, however, it is based on a secant stiffness formulation and currently utilizes only the lowest order finite elements. The procedure is adaptable to existing linear elastic algorithms and thus enables an easy conversion to nonlinear analysis capability.

RESEARCH SIGNIFICANCE

This paper shows that the response of reinforced concrete membrane structures can be predicted accurately using nonlinear finite element methods, provided they embody realistic constitutive relations for the

Received Sept. 18, 1987, and reviewed under Institute publication policies.

ACI member Frank J. Vecchio is an assistant professor in the Department of Civil Engineering at the University of Toronto, Ontario, Canada. He is on a leave of absence from Ontario Hydro, where he was involved in the analysis and design of reinforced concrete nuclear power plant structures. Dr. Vecchio is a member of ACI Committee 435, Deflection of Concrete Building Structures, and of Canadian Standard Association CSA-N287.3, Technical Committee on Concrete Containment Structures for Nuclear Power Plants.

component materials. Further, it is shown that such analyses can be performed by simple modification of existing linear elastic routines, and that modifications based on a secant stiffness formulation using simple low-powered elements are viable alternatives to more complex formulations.

STRESS-STRAIN RELATIONSHIPS

The finite element procedure herein is made to reflect the nonlinear behavior of reinforced concrete by adopting the formulations of the MCFT. The MCFT, described in Reference 2, is an analytical model for reinforced concrete membranes based on a smeared crack approach in which the cracked concrete is treated as a new material with unique stress-strain characteristics. Equilibrium, compatibility, and stress-strain relationships are formulated in terms of average stresses and average strains, but local stress conditions at crack locations are also given consideration. The stress-strain formulations of the MCFT have been applied to a variety of concrete structural analysis problems (e.g., References 12 through 14) and typically have yielded excellent agreement with experimental results.

Consider an orthogonally reinforced concrete membrane element as shown in Fig. 2(a). The element contains smeared reinforcement in the longitudinal (x) and transverse (y) directions, with the amounts given by the reinforcement ratios ρ_x and ρ_y and the yield strengths by f_{xy} and f_{yy}, respectively. The concrete is characterized by a cylinder compressive strength f'_c, a strain at peak stress ϵ_o, and a tensile cracking stress f_{cr}. Loads acting on the element's edge planes are assumed to consist of the uniform axial stresses f_x and f_y and the uniform

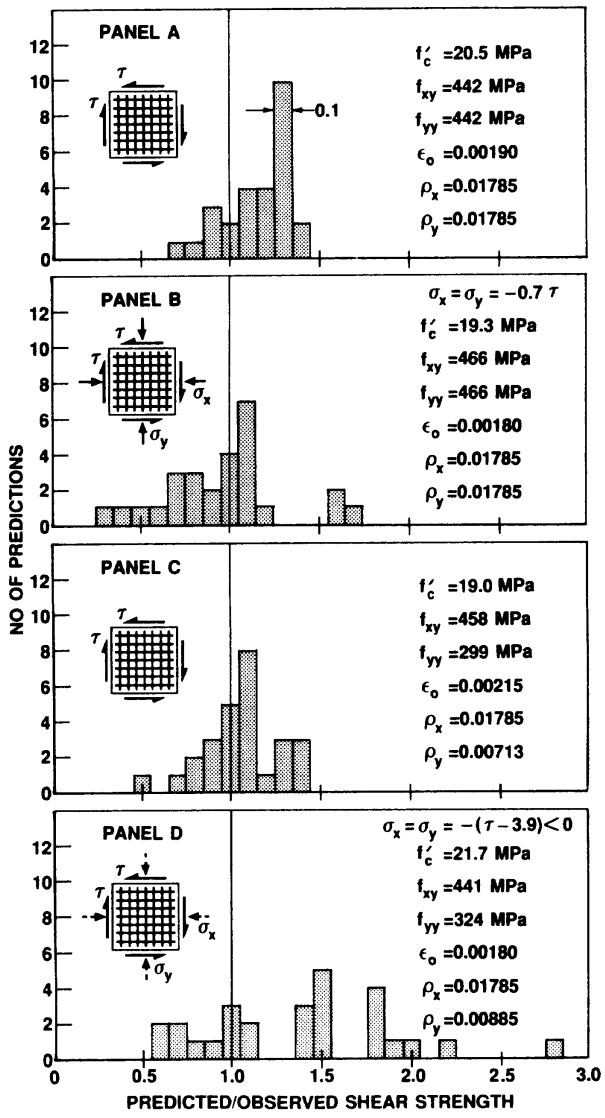

Fig. 1—Scatter in predicted strengths of panels received in international prediction competition

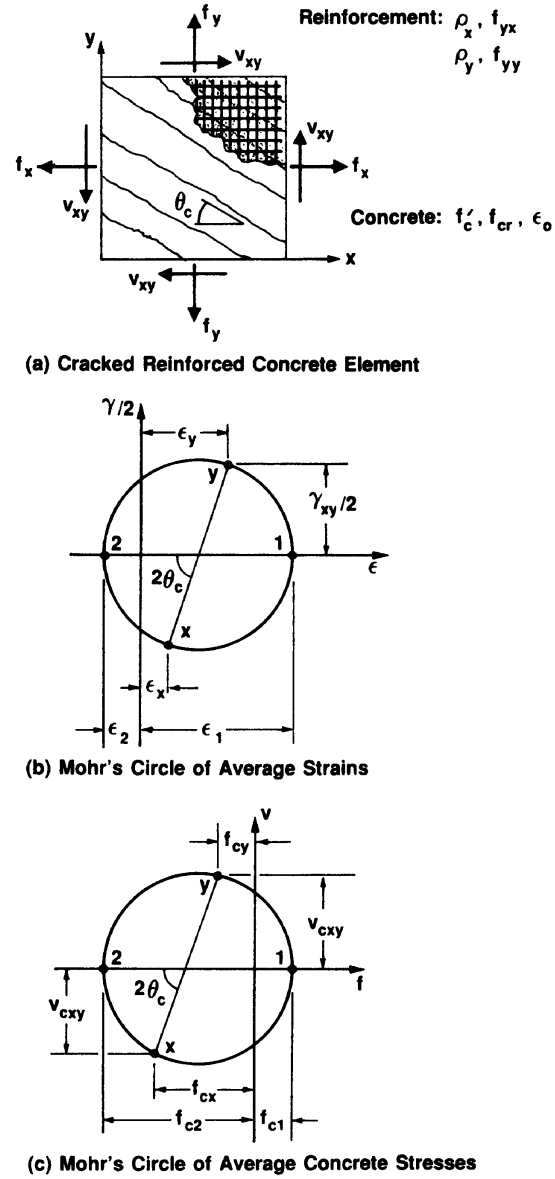

Fig. 2—Average stress and strain conditions defined for a membrane element

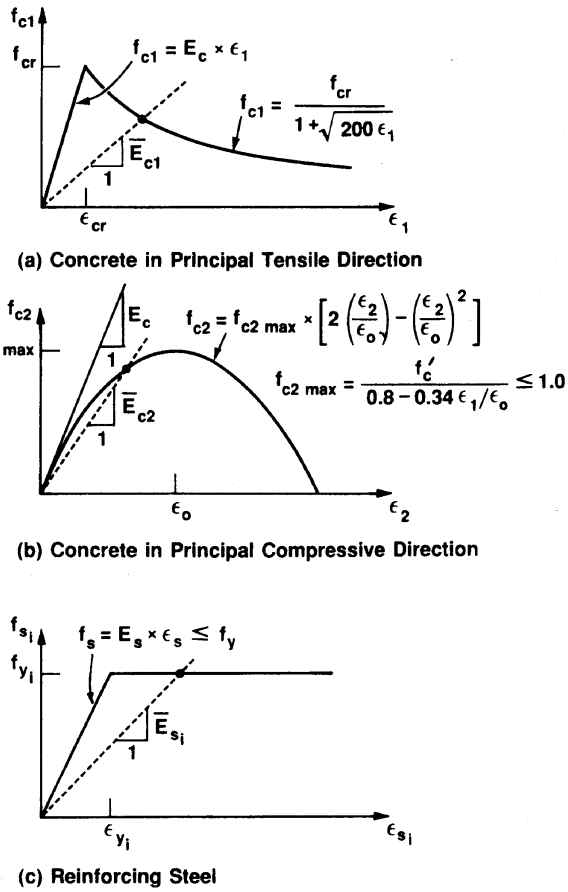

Fig. 3—Constitutive relations and secant moduli used in analysis procedure

shear stress v_{xy}. Deformation of the element is assumed to occur such that the edges remain straight and parallel.

Under the acting loads, an equilibrium condition is attained resulting in a unique strain condition defined by the two normal strains ϵ_x and ϵ_y and the shear strain γ_{xy}. From a Mohr's circle construction [Fig. 2(b)], the principal tensile strain ϵ_1, the principal compressive strain ϵ_2, and the inclination of the strain field (i.e., crack direction) θ_c can be found

$$\epsilon_1 = \tfrac{1}{2}(\epsilon_y + \epsilon_x) + \tfrac{1}{2}[(\epsilon_y - \epsilon_x)^2 + \gamma_{yx}^2]^{1/2} \quad (1)$$

$$\epsilon_2 = \tfrac{1}{2}(\epsilon_y + \epsilon_x) - \tfrac{1}{2}[(\epsilon_y - \epsilon_x)^2 + \gamma_{yx}^2]^{1/2} \quad (2)$$

$$\theta_c = \tfrac{1}{2}\tan^{-1}[\gamma_{xy}/(\epsilon_y - \epsilon_x)] \quad (3)$$

The stresses in the concrete and reinforcement are determined from the strains according to MCFT constitutive relations (Fig. 3). The principal compressive stress in the concrete f_{c2}, is

$$f_{c2} = f_{c2max} \cdot \left[2\left(\frac{\epsilon_2}{\epsilon_o}\right) - \left(\frac{\epsilon_2}{\epsilon_o}\right)^2\right] \quad (4)$$

where

$$f_{c2max} = \frac{-f'_c}{0.8 - 0.34\,\epsilon_1/\epsilon_o} \quad (5)$$

This formulation reflects the strain softening effect prevalent in cracked concrete in compression.

For concrete in tension, prior to cracking, a linear stress-strain relation is used. Thus, the principal tensile stress f_{c1} is

$$f_{c1} = E_c \cdot \epsilon_1,\ \epsilon_1 \leq \epsilon_{cr} \quad (6)$$

where E_c is the initial tangent modulus of elasticity of the concrete ($E_c = 2f'_c/\epsilon_o$), and ϵ_{cr} is the cracking strain. After cracking, the following relation is suggested to reflect tension stiffening effects

$$f_{c1} = f_{cr}/(1 + \sqrt{200 \cdot \epsilon_1}) \quad (7)$$

To insure that the concrete average tensile stress can be transmitted across cracks, f_{c1} is subject to the following upper limit

$$f_{c1} \leq \rho_x (f_{yx} - f_{sx}) \cdot \sin^2\theta_c + \rho_y (f_{yy} - f_{sy}) \cdot \cos^2\theta_c \quad (8)$$

where f_{sx} and f_{sy} are reinforcement stresses.

Stresses in the reinforcement are determined using elastic-plastic stress-strain relations. Thus

$$f_{sx} = E_s \cdot \epsilon_x \leq f_{yx} \quad (9)$$

$$f_{sy} = E_s \cdot \epsilon_y \leq f_{yy} \quad (10)$$

where E_s is the elastic modulus of the reinforcement steel. Eq. (9) and (10) can be modified to allow for strain hardening or prestressing, if necessary.

The principal average stresses in the concrete and Mohr's circle approach [see Fig. 2(c)] are then used to determine the concrete stresses in the x- and y-directions f_{cx} and f_{cy} respectively, and the concrete normal shear stress v_{cxy}

$$f_{cx} = \tfrac{1}{2}(f_{c1} + f_{c2}) - \tfrac{1}{2}(f_{c1} - f_{c2}) \cdot \cos 2\theta_c \quad (11)$$

$$f_{cy} = \tfrac{1}{2}(f_{c1} + f_{c2}) + \tfrac{1}{2}(f_{c1} - f_{c2}) \cdot \cos 2\theta_c \quad (12)$$

$$v_{cxy} = \tfrac{1}{2}(f_{c1} - f_{c2}) \cdot \sin 2\theta_c \quad (13)$$

The stresses in the concrete and in the reinforcement should be in equilibrium with the known loads f_x, f_y, and v_{xy} acting on the element. That is

$$f_{cx} + \rho_x \cdot f_{sx} = f_x \quad (14)$$

$$f_{cy} + \rho_y \cdot f_{sy} = f_y \quad (15)$$

and

$$v_{cxy} = v_{xy} \quad (16)$$

In a MCFT element analysis, if Eq. (14) through (16) are not satisfied, then the assumed strain state ϵ_x, ϵ_y, γ_{xy} is considered incorrect and must be revised. In finite

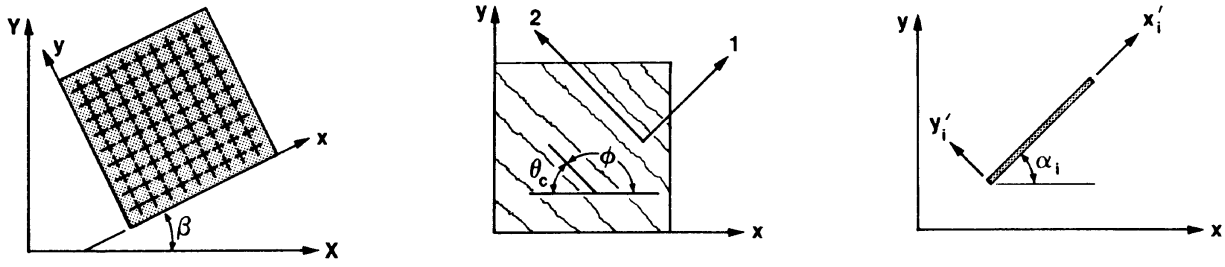

(a) Element in Global System (b) Concrete Component (c) Reinforcement Components

Fig. 4—Coordinate reference systems

element analysis, these local equilibrium checks are not performed directly.

Given compatible stress and strain fields, secant moduli can be defined for the concrete and reinforcement (shown in Fig. 3). Values required in the finite element formulations to come include the following

$$\bar{E}_{c1} = f_{c1}/\epsilon_1 \tag{17}$$

$$\bar{E}_{c2} = f_{c2}/\epsilon_2 \tag{18}$$

$$\bar{E}_{sx} = f_{sx}/\epsilon_x \tag{19}$$

$$\bar{E}_{sy} = f_{sy}/\epsilon_y \tag{20}$$

where $\bar{E}_{c1}$ and $\bar{E}_{c2}$ relate to the stress-strain behavior of the concrete in the principal directions, and $\bar{E}_{sx}$ and $\bar{E}_{sy}$ relate to the reinforcement in the two orthogonal directions.

FINITE ELEMENT PROCEDURE

With minor modifications, existing linear elastic finite element routines can be made to incorporate the stress-strain formulations previously presented and thus can be converted to nonlinear analysis capability. Development of linear elastic procedures is well documented in the literature, with References 11, 15, and 16 having been particularly useful. The emphasis here will be on the modifications required.

In constructing an element stiffness matrix [k], the material stiffness [D] is required to relate stresses $\{f\}$ to strains $\{\epsilon\}$, that is

$$\{f\} = [D]\{\epsilon\} \tag{21}$$

where

$$\{f\} = \begin{Bmatrix} f_x \\ f_y \\ v_{xy} \end{Bmatrix} \text{ and } \{\epsilon\} = \begin{Bmatrix} \epsilon_x \\ \epsilon_y \\ \gamma_{xy} \end{Bmatrix}$$

For a linear elastic isotropic material, in a plane stress state

$$[D] = \frac{E}{1-\nu^2}\begin{bmatrix} 1 & \nu & 0 \\ \nu & 1 & 0 \\ 0 & 0 & (1-\nu)/2 \end{bmatrix} \tag{22}$$

To reflect the nonlinear behavior of reinforced concrete as defined previously, matrix [D] must be modified.

Assume that the global reference system is measured in X, Y space and that the element reference axes are x, y as defined in Fig. 4. Further, the reinforcement orientations within the element are measured in x_i', y_i' axes systems. The angles β, ϕ, and α_i are used to relate directions.

The material stiffness matrix [D] for the element is defined with respect to the global X, Y axes by first defining relations for the concrete component $[D]_c$ and for each of the reinforcement components $[D]_{si}$. The total stiffness matrix is then determined by combining the component stiffness matrixes, using appropriate transformations to take into account the directional dependence of the materials. Thus

$$[D] = [T]^T [D]_c [T] + \sum_i [T]^T [D]_{si} [T] \tag{23}$$

Note that [T] will differ for each of the components.

According to the MCFT, cracked concrete can be considered as an orthotropic material with its principal axes[1,2] corresponding to the direction of the principal tensile strain and principal compressive strain, respectively. Further, after cracking, Poisson's effect can be considered to be negligible. Thus, the concrete material stiffness matrix $[D]_c$ evaluated with respect to the principal 1, 2 axes system is

$$[D]_c = \begin{bmatrix} \bar{E}_{c2} & 0 & 0 \\ 0 & \bar{E}_{c1} & 0 \\ 0 & 0 & \bar{G}_c \end{bmatrix} \tag{24}$$

where

$$\bar{G}_c \approx (\bar{E}_{c1} \cdot \bar{E}_{c2})/(\bar{E}_{c1} + \bar{E}_{c2}) \tag{25}$$

and where $\bar{E}_{c1}$ and $\bar{E}_{c2}$ are the secant moduli as evaluated using Eq. (17) and (18) for a particular stress/strain state.

For each reinforcement component, a reinforcement material stiffness matrix $[D]_{si}$ is evaluated as follows

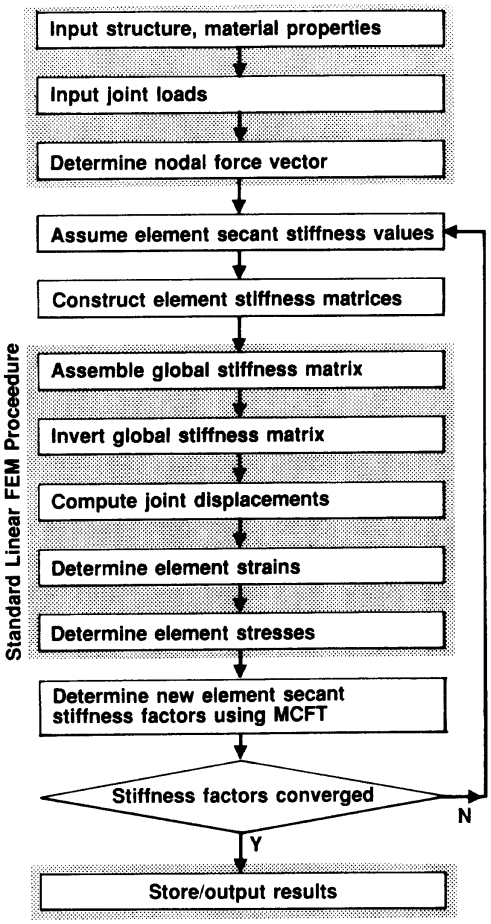

Fig. 5—Flowchart for nonlinear finite element procedure

$$[D]_{si} = \begin{bmatrix} \rho_i \cdot \bar{E}_{si} & 0 & 0 \\ 0 & 0 & 0 \\ 0 & 0 & 0 \end{bmatrix} \quad i = x, y \tag{26}$$

where $\bar{E}_{si}$ is the secant moduli for the reinforcement steel, again as determined for a particular stress/strain state using Eq. (19) and (20). Note that the previous formulation makes no allowance for dowel action although the possibility to do so exists. Also note that the formulation presented here is for orthogonally reinforced panels (i.e., $i = x, y$) but can be generalized to include arbitrary reinforcement patterns.

The transformation matrix $[T]$ to be used in Eq. (23) is given[17] by

$$[T] = \begin{bmatrix} \cos^2\psi & \sin^2\psi & \cos\psi\sin\psi \\ \sin^2\psi & \cos^2\psi & -\cos\psi\sin\psi \\ -2\cos\psi\sin\psi & 2\cos\psi\sin\psi & (\cos^2\psi - \sin^2\psi) \end{bmatrix} \tag{27}$$

where, for the concrete component

$$\psi = \phi + \beta = 180 - \theta_c + \beta \tag{28}$$

and for the reinforcement components

$$\psi = \alpha_i + \beta \tag{29}$$

Having determined the matrix $[D]$, the element stiffness matrix $[k]$ can then be evaluated. Standard procedures can be used, as described in Reference 11 and dependent on the order of the finite element involved, but summarized as

$$[k] = \int [B]^T [D][B]\, dV \tag{30}$$

where $[B]$ is dependent on the assumed element displacement functions. For triangular and rectangular plane stress elements based on linear displacement functions, the coefficients of the stiffness matrix can be evaluated using closed-form expressions,[18] eliminating costly numerical integration procedures. It should be noted that the element stiffness matrixes and the global stiffness matrix $[K]$ remain symmetric matrixes.

By using the modified elastic procedures in an iterative manner, progressively refining the calculated material stiffness matrixes $[D]$ for each element, a nonlinear analysis can be effected. The algorithm suggested is summarized in Fig. 5. First, the structure properties (e.g., joint coordinates, element indexes, support conditions, etc.) and material properties (e.g., concrete strength, reinforcement orientation, percentage and strength, element thickness, etc.) are defined. Next, joint loads or distributed element loads are input and a nodal force vector $\{R\}$ is calculated. Secant stiffness values for the materials in each element (i.e., $\bar{E}_{c1}$, $\bar{E}_{c2}$, $\bar{E}_{sx}$, $\bar{E}_{sy}$) are estimated and the material stiffness matrixes $[D]$ are computed. For the first iteration, the coefficients for an uncracked isotropic material [i.e., as given in Eq. (22)] can be used. The element stiffness matrixes $[k]$ for each element are calculated using Eq. (30), and the structure stiffness matrix $[K]$ is assembled. The matrix $[K]$ is then inverted, and the unknown nodal point displacements $\{r\}$ are found

$$\{r\} = [K]^{-1}\{R\} \tag{31}$$

From the joint displacements, the element strains and element stresses are determined

$$\{\epsilon\} = [B]\{r\} \tag{32}$$

$$\{f\} = [D]\{\epsilon\} \tag{33}$$

For each element, knowing the strains, new secant moduli ($\bar{E}_{c1}$, $\bar{E}_{c2}$, $\bar{E}_{sx}$, and $\bar{E}_{sy}$) are calculated using Eq. (1) through (10), and Eq. (17) through (20). A new material stiffness matrix $[D]'$ is determined for each element using Eq. (23) through (29). If the material stiffness matrixes have not converged, that is if $[D]' \neq [D]$, then $[D]'$ can be used as the new estimate and the analysis is repeated. After several iterations, the calculated values will converge and final results can be obtained.

This procedure was implemented into an existing linear elastic finite element code, with the resulting program named TRIX. Approximately 100 man-hours were required to effect fully the conversion. TRIX utilizes a 6-deg-of-freedom plane stress triangle (CST) and an

8-deg-of-freedom plane stress rectangle (PSR) to model membrane elements. In addition, a 4-deg-of-freedom truss bar element is available for modeling discrete reinforcing bars. Explicit stiffness matrix formulations for the CST and PSR elements, and detailed calculations for an example analysis, are given in Reference 18.

EXPERIMENTAL CORROBORATION

Experimental results were examined to obtain an indication of the accuracy of the proposed procedure. Three substantially different types of test specimens were analyzed using TRIX, and the results were compared to the observed behaviors. As well, the predicted responses obtained using the more complex program FIERCM were also examined for comparative purposes. (Note that FIERCM, also based on the MCFT, utilizes a tangent stiffness formulation, higher order elements, and a substantially different tension stiffening model.)

Bhide and Collins[19] reported a test series involving 31 panels loaded under various combinations of tension and shear. Panel PB21, shown in Fig. 6(a), was heavily reinforced in one direction ($\rho_x = 0.02195$) but not reinforced in the transverse direction ($\rho_y = 0$). Uniformly applied edge loads resulted in a ratio of uniaxial tensile stress to shear stress of 3.1:1 (i.e., $f_x = 3.1\ v_{xy}$, $f_y = 0$). Loads were monotonically increased in constant ratio until failure occurred.

Since the material properties and stress conditions were uniform throughout, one element was sufficient to model the structure [see Fig. 6(b)]. Nevertheless, the panel represented a severe test for any analysis procedure since predicted behavior is highly dependent on the assumed constitutive relations for concrete. The lack of reinforcement in the transverse direction further tests the numerical stability of the procedure.

The predicted response for Panel PB21 obtained from a TRIX analysis is compared to the observed behavior in Fig. 6(c). [Note that theoretical behavior is marked by a smooth transition from uncracked to cracked conditions due to the tension stiffening formulation used, i.e., Eq. (7)]. Good agreement is seen both in terms of load-deformation response and ultimate strength. The ratio of the experimental to predicted shear strength is 1.08. The response predicted by FIERCM is significantly weaker, with a ratio of experimental to predicted shear strength of 1.32. Bhide, in modifying the MCFT to account for dowel action and crack slip, reports a strength ratio of 1.05 for this panel.

A deep beam tested by Leonhardt and Walther,[20] shown in Fig. 7(a), was also examined. The beam was 1600 mm (63 in.) square and 100 mm (4 in.) thick in dimension, was simply supported along the bottom edge, and was subjected to a uniformly distributed load along the top. Vertical reinforcement was uniform throughout ($\rho_y = 0.00175$). The horizontal reinforcement was heavier in the lower regions ($\rho_x = 0.01787$) and lighter above ($\rho_x = 0.00175$). This specimen represented a membrane structure with smeared reinforcement whose

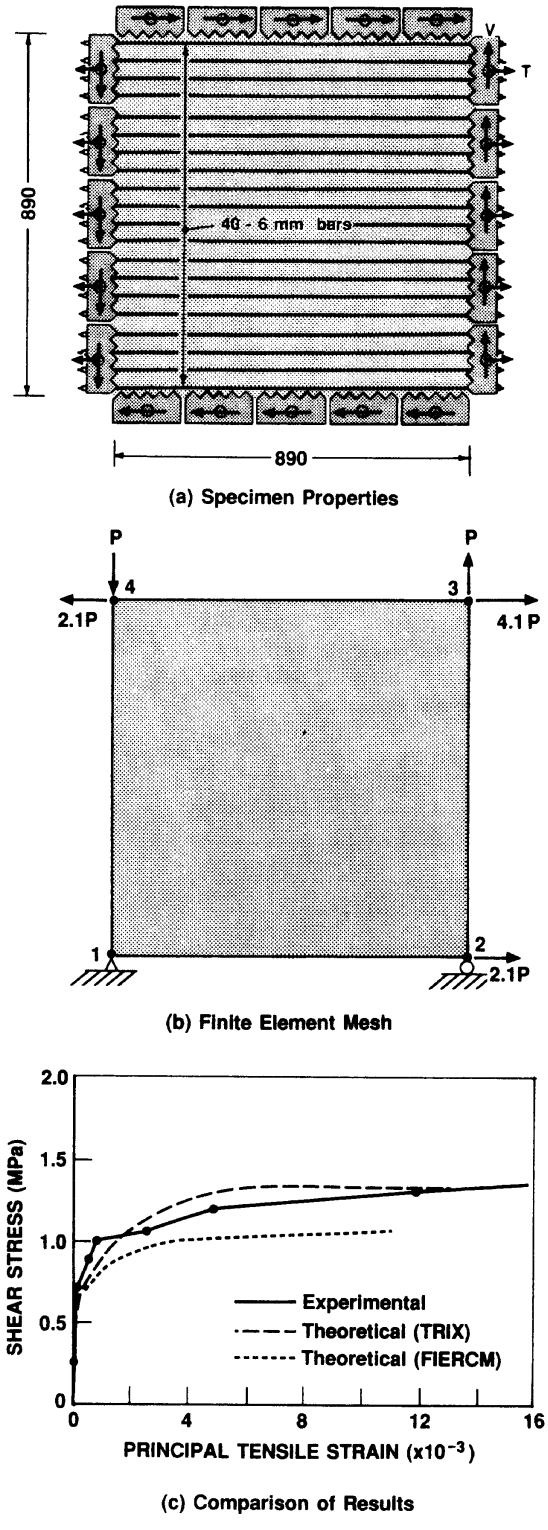

Fig. 6—Analysis of Bhide panel specimen PB21 (25.4 mm = 1 in.; 6.895 MPa = 1 ksi)

behavior would be dependent on the nonuniform nature of the stress and strain fields generated within. For analysis, using symmetry, half the beam was modeled using 128 rectangular elements [see Fig. 7(b)].

Shown in Fig. 7(c) is the observed response of the beam in terms of the midspan deflection against the total load applied. The response predicted using TRIX, also shown in Fig. 7(c), closely approximates the ob-

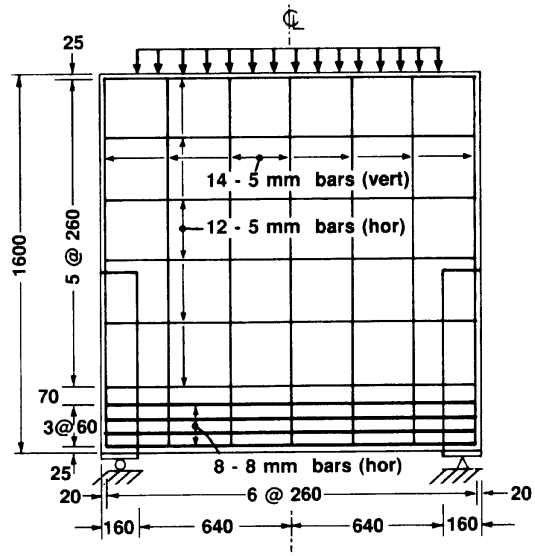

Thickness, t =100 all dimensions in mm

Concrete: f'_c =29.6 MPa, ϵ_o =0.002
5 mm bars: f_y =415 MPa, A_s =20 mm^2
8 mm bars: f_y =415 MPa, A_s =54 mm^2

(a) Specimen Properties

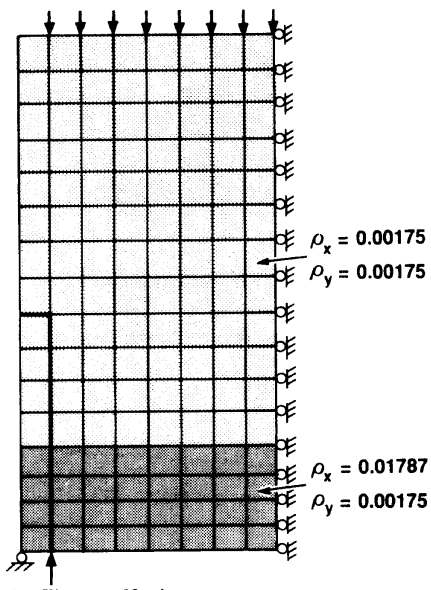

(b) Finite Element Mesh

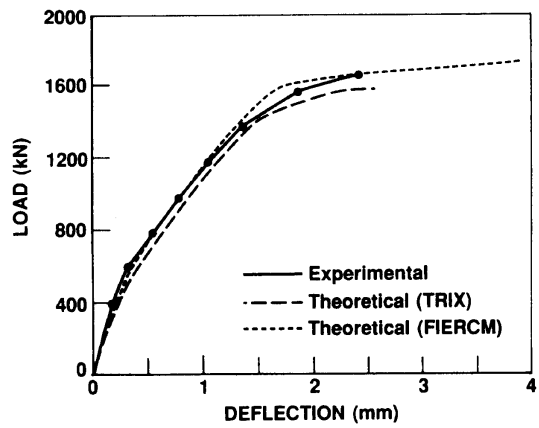

(c) Comparison of Results

Fig. 7—Analysis of Leonhardt and Walther deep beam specimen. (25.4 mm = 1 in.; 6.895 MPa = 1 ksi; 4.448 kN = 1 kip)

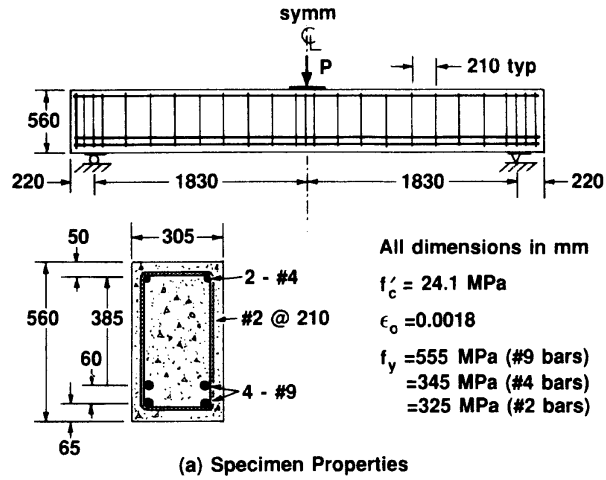

(a) Specimen Properties

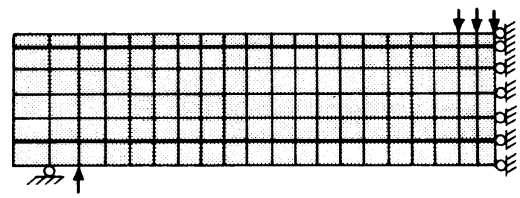

(b) Finite Element Mesh

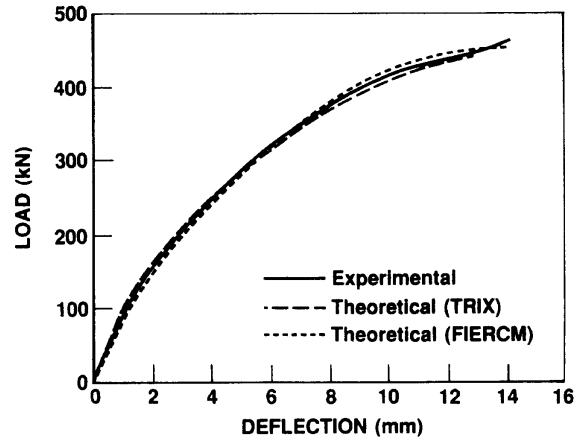

(c) Comparison of Results

Fig. 8—Analysis of Bresler and Scordelis shear beam A1 (25.4 mm = 1 in.; 6.895 MPa = 1 ksi; 4.448 kN = 1 kip)

served behavior. Aspects of response pertaining to strength, stiffness, cracking patterns, reinforcement stresses, and concrete distress regions were all in good agreement. Also shown is the response predicted using FIERCM, which correlates equally well.

One in a series of beams tested by Bresler and Scordelis[21] was also examined. Beam A-1, described in Fig. 8(a), was heavily reinforced with bottom longitudinal steel but lightly reinforced with transverse steel. Thus, the beam was designed to experience a concrete shear failure when simply supported and subjected to a concentrated load at the midspan. The beam was modeled using 120 rectangular elements and 40 truss bar elements [see Fig. 8(b)]. The longitudinal reinforcement was modeled in a discrete manner using the bar elements, while the shear reinforcement was included in

the properties of the rectangular elements and thus modeled in a smeared manner. This case differs from the Leonhardt and Walther deep beam in that the nonuniformly distributed reinforcement had to be modelled discretely and that flexural behavior was a major influencing factor.

Shown in Fig. 8(c) are the predicted and observed load-deflection response curves for Beam A-1. Again, the behavior predicted using TRIX is seen to accurately model the actual response. Cracking patterns and reinforcement strains were also in close agreement. The response predicted by FIERCM, using rectangular elements based on cubic displacement distributions, is no more accurate.

One final comparison can be made with respect to the failure loads of the four test panels from the prediction competition.[1] While many complex nonlinear finite element procedures were used by various researchers, the best set of predictions was made by Cervenka using a simple tangent stiffness formulation. For the four panels, the mean of the ratio of experimental to predicted ultimate shear stress obtained by Cervenka was 0.91. Using TRIX, based on the procedures described in this report, the accuracy of the predictions is significantly improved to where the ratio is 0.98. Using the more complex FIERCM routine, a mean ratio of 0.99 is obtained.

APPLICATIONS

The procedure described is applicable to the analysis of reinforced concrete structures in which a plane stress state can be assumed. The structure reinforcement and resulting crack pattern should be well distributed, and the acting loads should be short-term and monotonic. The procedure should not be used in structures where a single crack dominates response or where dowel action, bond slip, or previous loading have a significant influence.

As an example application, the procedure will be used to analyze the response of a reinforced concrete wall containing a small square-shaped perforation. A wall portion 850 mm (33.5 in.) square and 70 mm (2.75 in.) thick will be assumed, with a 150 mm^2 (6 in.^{2}) perforation at the center [see Fig. 9(a)]. Reinforcement is assumed uniform in the vertical and horizontal direction, both at a reinforcement ratio of 0.015. The concrete strength is 25 MPa (3.625 ksi), and the reinforcement strength is 400 MPa (58 ksi). The wall is subjected to pure shear loads. The finite element model used to represent one-quarter of the structure is shown in Fig. 9(b). A total of 12 rectangular elements and 28 triangular elements were used, and all reinforcement was modeled in a smeared manner accounted for in the membrane element specifications.

Two analyses were made of the perforated wall element. In the first, reinforcement interrupted by the opening was replaced in an equal amount by reinforcement placed to either side with appropriate provisions made for development length. This is roughly in accordance with the guidelines of ACI Committee 313,[22] which recommends that 120 percent of the interrupted reinforcement be replaced. In the second analysis, the interrupted reinforcement was not replaced. Also, a third analysis was conducted using a single-element model to determine the behavior of the wall if it were

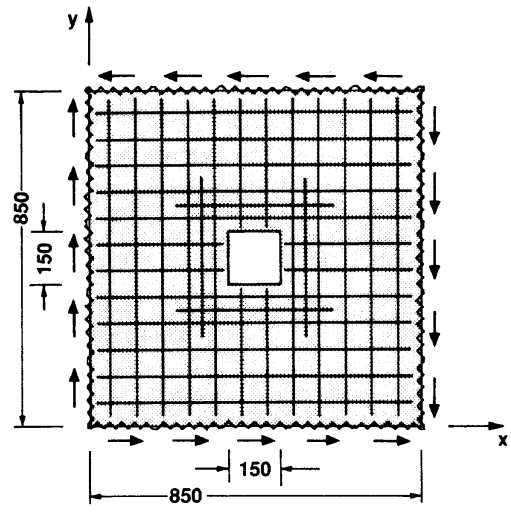

All dimensions in mm
Thickness, t = 70 mm
Concrete: f'_c = 25 MPa ϵ_o = 0.002
Reinforcement: ρ_x = 0.0150 f_y = 400 MPa
ρ_y = 0.0150 f_y = 400 MPa

(a) Element Properties

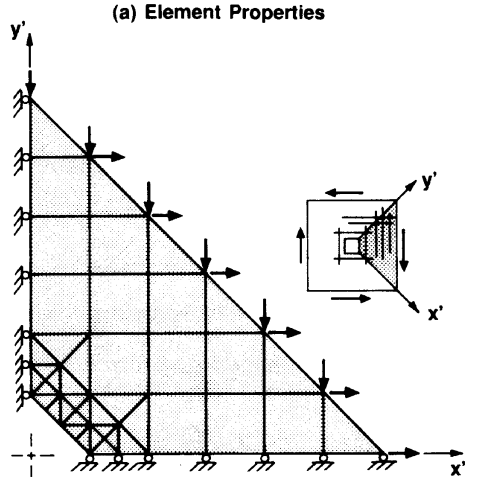

(b) Finite Element Mesh

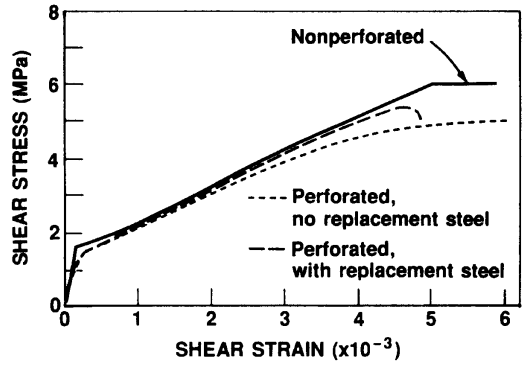

(c) Predicted Response

Fig. 9—Analysis of hypothetical wall specimen with perforation (25.4 mm = 1 in.; 6.895 MPa = 1 ksi)

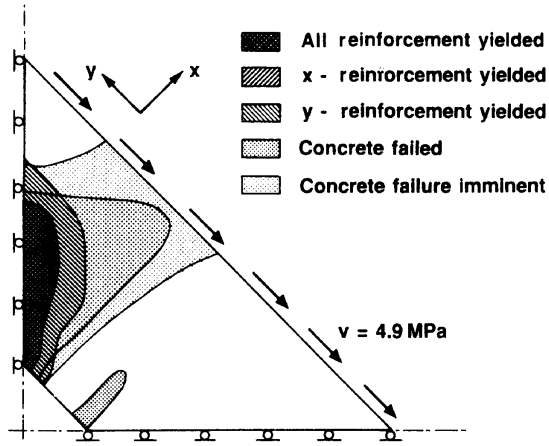

(a) Perforated Panel with no Replacement Steel

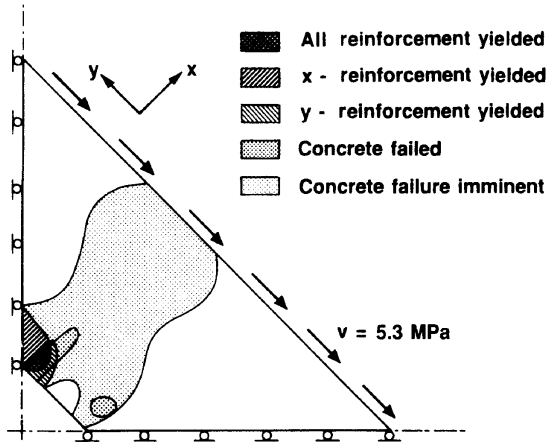

(b) Perforated Panel with Replacement Steel

Fig. 10—Predicted damage in perforated wall elements just prior to failure (6.895 MPa = 1 ksi)

not perforated. The load-deformation responses determined for all three are shown in Fig. 9(c). Note that the shear stress shown is the nominal stress applied uniformly along the boundary edges and that the shear strains are average values determined over the entire area of the wall element.

The nonperforated wall structure experiences a linear response up to the cracking stress of 1.65 MPa (0.240 ksi). Beyond cracking, there is a gradually softening response as the tension stiffening effect is reduced. Due to the geometry and loading, stresses and strains are uniform throughout at all times. At a shear stress of 6.0 MPa (0.870 ksi), a ductile failure occurs as the horizontal and vertical reinforcement yield simultaneously at all points within the wall panel.

In the perforated wall element not having replacement steel, first cracking occurs around the top corner of the perforation at a shear stress of 0.55 MPa (0.080 ksi). As loading continues, cracking becomes more widespread but is most severe around the opening. First yielding of the vertical reinforcement (in the quarter model) occurs at a shear stress of 2.5 MPa (0.360 ksi), followed by first yielding of the horizontal reinforcement at a shear stress of 3.3 MPa (0.480 ksi). Local crushing of the concrete is first experienced at a shear stress of 3.7 MPa (0.540 ksi). As loads increase, the zones of yielding and crushing spread, and at 4.9 MPa (0.710 ksi) shear, the distress regions are fairly widespread, as shown in Fig. 10(a). At a shear stress of 4.99 MPa (0.720 ksi), a ductile shear failure of the concrete occurs across the element. The overall stiffness of the wall element as compared to the nonperforated wall is noticeably weaker, as evident in Fig. 9(c).

In the perforated wall with replacement steel added, cracking again begins at a shear stress of 0.55 MPa (0.080 ksi) with a subsequent reduction in wall stiffness. First yielding of the vertical reinforcement occurs at a shear stress of 3.5 MPa (0.510 ksi), first yielding of the horizontal reinforcement occurs at 4.3 MPa (0.620 ksi), and first local crushing of the concrete occurs at 4.9 MPa (0.710 ksi) shear. These distress zones are limited to small regions in the vicinity of the opening and occur at significantly higher load levels than in the wall having no added reinforcement. At a shear stress of 5.3 MPa (0.770 ksi), just before failure, the damage zones are still relatively minor [see Fig. 10(b)] and would be perhaps imperceptible. At a shear stress of 5.4 MPa (0.780 ksi), a brittle failure of the wall occurs by crushing shear failure of the concrete.

Thus, although all interrupted reinforcement is replaced, the element behavior is significantly altered by the presence of an opening. Not only is the stiffness and ultimate load capacity reduced, but the failure mode is changed from that of a ductile yielding of reinforcement to one involving a sudden brittle failure of the concrete. Adding an additional 20 percent in replacement steel, as per ACI 313 guidelines, would not reverse the change in failure mode.

CONCLUSIONS

A nonlinear finite element procedure was developed to predict the response of reinforced concrete membrane elements. The procedure is based on a secant stiffness formulation, incorporating constitutive relations for concrete as derived from the modified compression field theory and utilizing only low order finite elements. Conclusions derived from the work include the following:

1. The response of reinforced concrete membrane structures can be predicted accurately using nonlinear finite element techniques.

2. Nonlinear finite element formulations can be simple enough such that currently existing linear elastic analysis programs can be converted readily to nonlinear analysis capability.

3. In developing a nonlinear formulation, the definition of realistic constitutive relations is more critical than the formulation of complex elements or solution procedures.

4. A secant stiffness approach can be as successful as the more common tangent stiffness approach, while being less restrictive on the nature of the constitutive relations that can be implemented or the solution procedures required.

5. Low-powered elements can be used in nonlinear analyses without unduly compromising accuracy, yet minimizing the potential for numerical stability problems.

6. Nonlinear finite element analysis can be a useful tool in investigating design details or the load-deformation response of reinforced concrete structures.

ACKNOWLEDGMENT

The work in this paper was made possible through funding from the Natural Sciences and Engineering Research Council of Canada, for which the author expresses his sincere gratitude.

NOTATION

E = modulus of elasticity of linear isotropic material
E_c = modulus of elasticity of concrete (initial tangent stiffness)
$\bar{E}_{c1}$ = secant modulus of concrete in principal tensile strain direction
$\bar{E}_{c2}$ = secant modulus of concrete in principal compressive strain direction
$\bar{E}_{sx}$ = secant modulus of reinforcement in x-direction
$\bar{E}_{sy}$ = secant modulus of reinforcement in y-direction
f'_c = compressive strength of concrete cylinder
f_{c1} = principal tensile stress in concrete
f_{c2} = principal compressive stress in concrete
f_{cr} = concrete cracking stress
f_{cx} = average stress in concrete in x-direction
f_{cy} = average stress in concrete in y-direction
f_{sx} = average stress in x-reinforcement
f_{sy} = average stress in y-reinforcement
f_x = element stress in x-direction
f_y = element stress in y-direction
f_{yx} = yield stress of x-reinforcement
f_{yy} = yield stress of y-reinforcement
$\bar{G}_c$ = secant shear modulus of concrete
v_{cxy} = shear stress on concrete, relative to x, y axes
v_{xy} = shear stress on element, relative to x, y axes
α = orientation of reinforcement relative to element x, y axes
β = orientation of element x, y axes relative to global X, Y axes
ϵ_1 = principal tensile strain in concrete
ϵ_2 = principal compressive strain in concrete
ϵ_o = strain in concrete cylinder at peak stress f'_c
ϵ_{cr} = strain in concrete at cracking
ϵ_x = strain in x-direction
ϵ_y = strain in y-direction
γ_{xy} = shear strain relative to x, y axes
θ_c = angle of inclination of principal stresses/strains in concrete
ϕ = orientation of crack direction relative to element x, y axes
ψ = characteristic angle in transformation matrix
ρ_x = steel reinforcement ratio in x-direction
ρ_y = steel reinforcement ratio in y-direction
[B] = element strain function matrix
[D] = composite material stiffness matrix
$[D]_c$ = concrete material stiffness matrix
$[D]_s$ = reinforcement material stiffness matrix
$\{\epsilon\}$ = element strain matrix
{f} = element stress matrix
[k] = element stiffness matrix
[K] = structure stiffness matrix
{r} = structure nodal displacement matrix
{R} = structure nodal force matrix
[T] = transformation matrix

REFERENCES

1. Collins, M. P.; Vecchio, F. J.; and Mehlhorn, G., "An International Competition to Predict the Response of Reinforced Concrete Panels," *Canadian Journal of Civil Engineering* (Montreal), V. 12, No. 3, Sept. 1985, pp. 626-644.

2. Vecchio, Frank J., and Collins, Michael P., "The Modified Compression-Field Theory for Reinforced Concrete Elements Subjected to Shear," ACI JOURNAL, *Proceedings* V. 83, No. 2, Mar.-Apr. 1986, pp. 219-231.

3. Vecchio, Frank J., and Collins, Michael P., "Predicting the Response of Reinforced Concrete Beams Subjected to Shear Using the Modified Compression Field Theory," *ACI Structural Journal,* V. 85, No. 3, May-June 1988, pp. 258-268.

4. "Design of Concrete Structures for Buildings," (CAN3-A23.3-M84), Canadian Standards Association, Rexdale, 1984, 281 pp.

5. Adeghe, L. N., "A Finite Element Model for Studying Reinforced Concrete Detailing Problems," PhD thesis, Department of Civil Engineering, University of Toronto, 1986, 264 pp.

6. Stevens, N. J.; Uzumeri, S. M.; and Collins, M. P., "Analytical Modelling of Reinforced Concrete Subjected to Monotonic and Reversed Loading," *Publication* No. 87-1, Department of Civil Engineering, University of Toronto, Jan. 1987, 201 pp.

7. Cook, William D., and Mitchell, Denis, "Studies of Disturbed Regions near Discontinuities in Reinforced Concrete Members," *ACI Structural Journal,* V. 85, No. 2, Mar.-Apr. 1988, pp. 206-216.

8. Barzegar-Jamshidi, F., and Schnobrich, W. C., "Nonlinear Finite Element Analysis of Reinforced Concrete under Short Term Monotonic Loading," Civil Engineering Studies, *Report* No. 530, University of Illinois, Urbana-Champaign, 1986, 137 pp.

9. Niwa, J.; Maekawa, K.; and Okamura, H., "Nonlinear Finite Element Analysis of Deep Beams," *Final Report,* IABSE Colloquium (Delft, 1981), International Association for Bridge and Structural Engineering, Zürich, 1981, pp. 335-350.

10. Bathe, K. Y., "A Finite Element Program for Automatic Dynamic Incremental Nonlinear Analysis," *MIT Report* No. 82448-7, Massachusetts Institute of Technology, Cambridge, 1977, 497 pp.

11. *Finite Element Analysis of Reinforced Concrete,* American Society of Civil Engineers, New York, 1982, 545 pp.

12. Ang, B. G., "Seismic Shear Strength of Circular Bridge Piers," PhD thesis, Department of Civil Engineering, University of Canterbury, Christchurch, 1985.

13. Mau, S. T., and Hsu, Thomas T. C., "Shear Behaviour of Reinforced Concrete Framed Wall Panels with Vertical Loads," *ACI Structural Journal,* V. 84, No. 3, May-June 1987, pp. 228-234.

14. Hsu, Thomas T. C., and Mo, Y. L., "Softening of Concrete in Torsional Members—Theory and Tests," ACI JOURNAL, *Proceedings* V. 82, No. 3, May-June 1985, pp. 290-303.

15. Yang, T. Y., *Finite Element Structural Analysis,* Prentice-Hall, Inc., Englewood Cliffs, 1986, 543 pp.

16. Weaver, William, Jr., and Johnston, Paul R., *Finite Elements for Structural Analysis,* Prentice-Hall, Inc., Englewood Cliffs, 1984, 403 pp.

17. Cervenka, Vladimir, "Constitutive Model for Cracked Reinforced Concrete," ACI JOURNAL, *Proceedings* V. 82, No. 6, Nov.-Dec. 1985, pp. 877-882.

18. Vecchio, F. J., "Reinforced Concrete Membrane Element Formulations," *Journal of Structural Engineering,* ASCE (submitted).

19. Bhide, S. B., and Collins, M. P., "Reinforced Concrete Elements in Shear and Tension," *Publication* No. 87-02, Department of Civil Engineering, University of Toronto, 1987, 147 pp.

20. Leonhardt, Fritz, and Walther, René, "Wandartige Träger," *Bulletin* No. 178, Deutscher Ausschuss für Stahlbeton, Berlin, 1966, 159 pp.

21. Bresler, Boris, and Scordelis, A. C., "Shear Strength of Reinforced Concrete Beams," ACI JOURNAL, *Proceedings* V. 60, No. 1, Jan. 1963, pp. 51-74.

22. ACI Committee 313, "Recommended Practice for Design and Construction of Concrete Bins, Silos, and Bunkers for Storage of Granular Materials (ACI 313-77) (Revised 1983)," American Concrete Institute, Detroit 1983, 21 pp. Also, *ACI Manual of Concrete Practice,* Part 4.